Generalized complex Swift-Hohenberg equation for optical parametric oscillators

Víctor J. Sánchez-Morcillo, Eugenio Roldán, and Germán J. de Valcárcel
Departament d'Òptica, Universitat de València, Dr. Moliner 50, 46100-Burjassot, Spain

Kestutis Staliunas
PTB Braunschweig, Laboratory 4.42, Bundesallee 100, 38116 Braunschweig, Germany
(Received 11 November 1996)

A generalized complex Swift-Hohenberg equation including diffraction and nonlinear resonance terms is derived for spatially extended nondegenerate optical parametric oscillators (OPOs) with flat end mirrors. For vanishing pump detuning this equation becomes the complex Swift-Hohenberg (SH) equation valid also for lasers. Nevertheless the similarities between OPOs and lasers are limited, since the diffractive character of OPOs is lost when the diffraction coefficients of signal and idler fields are equal. This manifests, e.g., in the absence of advection by traveling waves (TWs), a clear difference with lasers. When pump detuning is nonzero a nonlinear resonance develops, as it occurs in degenerate OPOs. This nonlinear resonance is essential in order to properly describe the TWs that OPOs support, and describes the bistability between TWs. This leads to the appearance of localized structures, which we also report here. [S1050-2947(97)05710-7]

PACS number(s): 42.65.Sf, 42.65.Yj, 47.32.Cc

I. INTRODUCTION

In spite of the complexity of most spatially extended nonlinear systems, many of them have been shown to be described, to a given degree of approximation, by a single variable (e.g., the electric-field amplitude in the case of optics), governed by a single partial differential equation, the so-called *order parameter equation* (OPE) (see, e.g., Ref. [1]). Prototypes of such OPEs are the Ginzburg-Landau and the Swift-Hohenberg (SH) equations, among others [1]. These equations play the role of paradigms since they describe the very basic mechanisms of pattern formation in many systems. Hence, the reason for finding OPEs is twofold. First, they capture the main properties of the system under study, thus allowing a simplified treatment of complex phenomena. Second, they can reveal the connections between very different pattern forming systems.

In the field of nonlinear optics, only two classes of OPEs have been obtained up to now, since Coullet *et al.* [2] derived a *complex* Ginzburg-Landau equation for a two-level laser model near its first threshold. They evidenced the interplay between diffraction *and* diffusion in the laser system, which is essential, for instance, for producing stable optical vortices, structures very similar to the spiral waves often observed in Belusov-Zhabotinsky reactions (e.g., Ref. [1]). A *real* Ginzburg-Landau equation was derived for optical bistability [3], for a singly resonant optical parametric oscillator [4], and for degenerate optical parametric oscillation [5]. In all cases, these Ginzburg-Landau equations were obtained for values of the cavity eigenfrequency exceeding the line-center frequency.

The second class of OPE that has been found in nonlinear optics is the SH equation or some of its generalizations. The *real* SH equation has been derived for degenerate optical parametric oscillation [5,6] and degenerate four-wave mixing [5]. Also that equation, with an additional constant term, has been derived for one-photon [3] and two-photon [7] optical bistability. The *complex* SH equation has been found in lasers [8,9], drift-type photorefractive oscillators [10], and nondegenerate optical parametric oscillation [6,11]. In all cases, these equations are valid for small values of the detuning (either positive or negative). As indicated in [3] the GL equation can be understood as a limiting case of the SH equation, and thus one can regard this equation as a model equation for pattern formation in nonlinear optics.

In the present paper we derive a generalized complex SH equation for nondegenerate optical parametric oscillation (OPO). Our result generalizes previous derivations of OPEs for this system [6,11] since we take explicitly into account the crucial influence of pump detuning.

Pattern formation in OPOs has been studied in the recent past, both in the degenerate and nondegenerate cases (in the following, when speaking about OPOs it should be understood that we mean nondegenerate OPOs, unless otherwise specified). Concerning the degenerate OPO the leading role of the roll (standing-wave) pattern in the spatiotemporal dynamics of the system has been shown [12,13], as well as the appearance of more complicated structures involving oscillations through a Hopf bifurcation for positive signal detuning [14], and the existence of localized structures [15,16]. The existence of a nonlinear resonance for large pump detuning was demonstrated and analyzed in detail in Ref. [5]. Various OPEs for this system were derived in [4,5,6,17] for different limiting cases.

The nondegenerate OPO has been studied previously in [4,6,11,13,18,19]. Longhi [18] has shown that OPO equations admit a family of traveling waves (TWs) that are exact solutions of the model. In this type of solution, signal and idler fields are each described by a TW. These two TWs are oppositely directed along the transverse plane (owing to momentum conservation), and have frequencies equally detuned, in opposite sides, from their reference frequencies (owing to energy conservation). Long-wavelength (phase) instabilities of the TWs were analyzed through a phase equation, and a numerical linear stability analysis of the TWs evidenced the existence of amplitude instabilities that affect

OPO TWs for low cavity losses for the pump field. Longhi has also shown, through the analysis of amplitude equations [19], that TWs are the winners in a TW-roll competition and that OPOs near threshold can support stable structures composed by the superposition of two perpendicularly oriented out-of-phase rolls, a state that gives rise to square intensity patterns.

The rest of this paper is organized as follows. In Sec. II the OPO model is presented and the linear stability analysis of the below-threshold solution is discussed briefly. In Sec. III the generalized complex SH equation is derived in the case of small effective cavity detuning. We comment on the analogy that exists between OPOs and lasers, and consider in detail the different limits of the equation. In Sec. IV some numerical results are reported. Finally in Sec. V a discussion about the ubiquity of the SH equation in nonlinear optics is made, and we consider the mechanism for the diffraction disappearance in the OPE.

II. OPO MODEL AND LINEAR STABILITY ANALYSIS OF THE BELOW THRESHOLD SOLUTION

We consider a nonlinear $\chi^{(2)}$ medium inside a plane resonator driven by a coherent field of amplitude E and frequency ω_L that propagates along the resonator axis z. The crystal converts the intracavity field of frequency ω_L and amplitude A_0 (pump) into two fields of frequencies $f_1\omega_L$ and $f_2\omega_L$ ($f_1+f_2=1$) and amplitudes A_1 (signal) and A_2 (idler), respectively. Three longitudinal modes of the cavity with frequencies $\omega_m (m=0,1,2)$ are assumed to be close to the frequencies $f_m\omega_L (f_0=1)$. The parameters of the model are the driving amplitude E, the detunings $\Delta_m=(\omega_m-f_m\omega_L)/\gamma_m$, the cavity decay rates γ_m, and the diffraction coefficients $a_m=c^2/2\gamma_m f_m\omega_L$, where c is the velocity of light.

The classical microscopic equations that describe this OPO system in the mean-field limit, in the paraxial and the single-longitudinal-mode approximations for each field are given in [4,13]. In order to make derivations simpler we define the following fields:

$$E=(1+i\Delta_0)P, \quad A_0=P+(1-i\Delta_0)X,$$

$$A_1=(1+\Delta_0^2)^{1/2}e^{i\omega_C t}Y, \quad A_2=(1+\Delta_0^2)^{1/2}e^{-i\omega_C t}Z, \quad (1)$$

where

$$\omega_C=(a_1\Delta_2-a_2\Delta_1)/a, \quad (2a)$$

$$a=(\gamma_1 a_1+\gamma_2 a_2)/(\gamma_1+\gamma_2). \quad (2b)$$

The inclusion of the pump detuning Δ_0 in definitions (1) is similar to that used in the study of degenerate OPOs [5]. This rescaling largely simplifies the derivation of the OPE of the system in the limit of large Δ_0, which is crucial in order to properly describe the dynamics of the system, as we show below. We also performed a change in the reference frequency ($+\omega_C$) in A_1 and ($-\omega_C$) in A_2 that just corresponds to eliminating the frequency shift of signal and idler fields at their generation threshold for a negative value of the *effective detuning parameter* [18]

$$\Delta=(\gamma_1\Delta_1+\gamma_2\Delta_2)/(\gamma_1+\gamma_2). \quad (2c)$$

In terms of the new variables the OPO model reads

$$\partial_t X=\gamma_0[-(1+i\Delta_0)(X+YZ)+i\tilde{a}_0\nabla^2 X], \quad (3a)$$

$$\partial_t Y=\gamma_1[-Y-i\tilde{a}_1(\Delta-\nabla^2)Y+PZ^*+i(1-i\Delta_0)XZ^*], \quad (3b)$$

$$\partial_t Z=\gamma_2[-Z-i\tilde{a}_2(\Delta-\nabla^2)Z+PY^*+i(1-i\Delta_0)XY^*], \quad (3c)$$

where X, Y, and Z are functions of time t and of the coordinates $\mathbf{r}=(x,y)$ on the plane transverse to the resonator axis, $\nabla^2=\partial_x^2+\partial_y^2$ is the transverse Laplacian (spatial coordinates have been normalized to $\sqrt{a}$), and $\tilde{a}_m=a_m/a$. We will consider the case of uniform driving field P and will take it as real and positive for definiteness.

The solution that characterizes OPO below signal and idler generation threshold is $X=Y=Z=0$. Its linear stability analysis against perturbations of the form $\exp[i(\mathbf{k}\cdot\mathbf{r}+\omega t)]$ shows that the trivial solution becomes unstable at $P=P_c$ being the largest growth perturbations (critical modes) those verifying $\mathbf{k}^2=k_C^2$ with [13]

$$P_C=\sqrt{1+\Delta^2}, \quad k_C^2=0 \quad \text{for} \quad \Delta\geqslant 0,$$

$$P_C=1, \quad k_C^2=-\Delta \quad \text{for} \quad \Delta\leqslant 0. \quad (4)$$

III. ORDER PARAMETER EQUATIONS FOR OPO

In this section we derive the OPE for OPOs, an equation that captures the basic space-time nonlinear dynamics of that system close to threshold, without limiting to any specific type of solution. We apply the same techniques that have allowed one to derive OPEs for other nonlinear optical systems, like optical bistability [3,7] lasers [9], degenerate optical parametric oscillators [5,6,17] and degenerate four-wave mixing [5]. In particular, we basically follow the same lines as in [5], which showed the necessity of explicitly considering the limit of large pump detuning Δ_0 in order to properly describe a degenerate OPO through an OPE.

A. Scalings and order-parameter equation

In order to derive OPEs one has to deal with ''slow'' space and time scales [1,20]. These scalings are suggested by the linear stability analysis of the bifurcating solution in the vicinity of which the behavior of the system is analyzed (in our case, the trivial solution). In the OPO case slow space scales arise either in the positive detuning Δ side (where the most unstable modes are centered around $\mathbf{k}=\mathbf{0}$) or in the small negative Δ side (where the most unstable modes have a small $|\mathbf{k}|$), see Eq. (4). In order to give a unified treatment of both situations we will thus consider small values (either positive or negative) of Δ, say $\Delta=O(\varepsilon)$ with ε a smallness parameter. Moreover, in this small detuning limit, the thresholds of instability of the trivial solution are close to each other [see also Eq. (4)], their difference being $O(\varepsilon^2)$. On the other hand, slow time scales occur when the pump parameter is varied in a small amount [say $O(\varepsilon^2)$] around its threshold value. Thus we adopt the scalings

$$\Delta=\varepsilon\delta,\quad P=1+\varepsilon^2 p,\quad k=\sqrt{\varepsilon}\kappa, \tag{5}$$

the latter defining a ''slow'' space, leading to the substitution

$$\nabla^2\rightarrow\varepsilon\nabla_1^2 \tag{6}$$

in Eqs. (3). In terms of the scalings (5), the eigenvalue λ with the largest real part (that which governs the instability of the trivial solution) reads, to the leading orders in the smallness parameter ε,

$$\gamma^{-1}\lambda=[(P-1)-\tfrac{1}{2}(\Delta+k^2)^2]-i[d(\Delta+k^2)], \tag{7}$$

where we have defined the parameters

$$\gamma=\frac{2\gamma_1\gamma_2}{\gamma_1+\gamma_2},\quad d=\frac{\widetilde{a}_1-\widetilde{a}_2}{2}. \tag{8}$$

Thus λ has an $O(\varepsilon^2)$ real part and an $O(\varepsilon)$ imaginary part. These two contributions to λ suggest the definition of two slow time scales $T_1=\varepsilon t$, $T_2=\varepsilon^2 t$, which using the chain rule for differentiation lead to the substitution

$$\partial_t\rightarrow\varepsilon\partial_{T_1}+\varepsilon^2\partial_{T_2} \tag{9}$$

in Eqs. (3) [21]. As occurs in the degenerate OPO case [5] the scaling of the pump detuning Δ_0 is not fixed by the linear stability analysis. In principle, one would consider the case $\Delta_0=O(1)$ as has been done in [6,11]. Nevertheless, this scaling for Δ_0 is unable to reproduce the well known bistability of the OPO solutions that affects, e.g., the uniform (space independent) steady state, for $\Delta_0\Delta>1$ (see, e.g., [18]). Thus, since Δ is assumed to be $O(\varepsilon)$, Δ_0 must be considered to be $O(\varepsilon^{-1})$ in order to cover this case. So we will further adopt the scaling

$$\Delta_0=\varepsilon^{-1}\delta_0. \tag{10}$$

Finally, we expand the fields as

$$X=\sum_{n=1}^{\infty}\varepsilon^n x_n,\quad Y=\sum_{n=1}^{\infty}\varepsilon^n y_n,\quad Z=\sum_{n=1}^{\infty}\varepsilon^n Z_n, \tag{11}$$

and substitute these expressions together with Eqs. (5), (6), (9), and (10) into Eqs. (3). This leads to an infinite hierarchy of linear problems at increasing orders in ε that can be easily, although nastily, solved. For the sake of brevity we do not give details of the derivation here, but only quote the most relevant results:

$$X=-YZ,$$

$$Z=Y^*-i(\Delta-\nabla^2)Y^*+i\Delta_0|Y|^2Y^*, \tag{12}$$

and Y is governed by the OPE

$$\begin{aligned}\gamma^{-1}\partial_t Y=&(P-1)Y-|Y|^2Y-id(\Delta-\nabla^2)Y-\tfrac{1}{2}(\Delta-\nabla^2\\&-\Delta_0|Y|^2)^2Y+\tfrac{1}{2}\Delta_0 Y(Y^*\nabla^2Y-Y\nabla^2Y^*)\\&+\Delta_0 d\,\frac{\gamma}{\gamma_2}\,[Y^2\nabla^2Y^*+Y^*(\vec{\nabla}Y)\cdot(\vec{\nabla}Y)\\&+2Y(\vec{\nabla}Y)\cdot(\vec{\nabla}Y^*)],\end{aligned} \tag{13}$$

where the parameters γ and d are given in Eq. (8). Notice that the fourth term on the right-hand side of Eq. (13), $(\Delta-\nabla^2-\Delta_0|Y|^2)^2Y$, expands as $(\Delta-\nabla^2-\Delta_0|Y|^2)[(\Delta-\nabla^2-\Delta_0|Y|^2)Y]$.

Let us just point out that in the OPE (13) $Y=\varepsilon y_1+\varepsilon^2 y_2$ is the signal field amplitude up to second order in ε, and that the OPE contains all terms up to the third order in ε, as in the laser case [9].

B. Case of small pump detuning: Relationships between OPOs and lasers

Before commenting on the general structure of Eq. (13) it is worth considering the limit of moderate (or null) pump detuning Δ_0. If $\Delta_0=0$, Eq. (13) becomes

$$\gamma^{-1}\partial_t Y=(P-1)Y-|Y|^2Y-id(\Delta-\nabla^2)Y-\tfrac{1}{2}(\Delta-\nabla^2)^2Y, \tag{14}$$

which is a complex Swift-Hohenberg equation, formally equivalent to that obtained for lasers [8,9]. This evidences the strong similarities existing between the space-time dynamics of OPOs and lasers when the OPO cavity is exactly resonant with the pump. If $\Delta_0=O(1)$ we obtain the same Eq. (14) since in this case all terms containing Δ_0 in Eq. (13) are $O(\varepsilon^4)$ or smaller, and thus can be ignored [note that $Y=O(\varepsilon)$, $\Delta=O(\varepsilon)$, and $\nabla^2=O(\varepsilon)$]. This complex SH equation (14) for OPOs has been previously obtained by us [11], making use of the same techniques described here, but considering the scaling $\Delta_0=O(1)$, and also independently by Longhi and Geraci [6]. Thus the generalized complex SH Eq. (13), although derived in the limit of large Δ_0, also describes OPO dynamics for small Δ_0.

Let us remark, however, that, even having been derived for $\Delta_0=O(1)$, Eq. (14) cannot be considered as a good description for OPOs in that limit, since the solutions given by it do not contain information on Δ_0. [Note that the OPE for OPOs derived in Ref. [6] is isomorphic to Eq. (14) with the substitution $Y\rightarrow\psi/\sqrt{1+\Delta_0^2}$. Thus Δ_0 appears only in a trivial way in the OPE derived by Longhi and Geraci, not affecting the OPO solutions' properties.] This is a serious defect since the traveling waves obtained from the original microscopic equations (3) always depend on Δ_0 [18] (and not only through a scaling factor), as we discuss in the following subsection.

With respect to the analogy between lasers and OPOs (strictly valid in the case $\Delta_0=0$), there is a fundamental difference between Eq. (14) and the corresponding equation for lasers. In the latter case, the diffractive contribution [the one corresponding to the third right-hand side (rhs) term in Eq. (14)] is always present [8,9], whereas in the OPO case it vanishes if the diffraction coefficients of signal and idler fields are equal, since in this case $d=0$ [see Eq. (8)] [this

also applies, obviously, to the complete OPE (13)]. This implies that one can deal with OPOs with or without diffractive features (we will come back to this effect in Sec. V). One of these features concerns the advection processes [20] brought about by TWs: if diffraction is present, any perturbation of a TW (e.g. an optical vortex [2]) moves (is advected) with a velocity proportional to d; in the case that $d=0$ vortices are at rest, and this results in a clear difference between lasers and OPOs, which we will discuss in Sec. IV A.

C. The general case: Nonlinear resonance and traveling waves

If we do not impose limitations on the values of the diffraction coefficient d and on the pump detuning parameter Δ_0, Eq. (13) is a generalized complex Swift-Hohenberg equation. A major difference between the complex SH equation (14) and Eq. (13) is the presence of a nonlinear resonance [fourth r.h.s. term in Eq. (13)]. This term is analogous to that found in degenerate OPOs [5] and is capable of reproducing the structure of the TWs of OPOs and, in particular, their bistability with the trivial solution. If a TW solution of the form $Y=|Y|\exp[i(\omega t+\mathbf{k}\cdot\mathbf{r})]$ is inserted into Eq. (13) one easily obtains

$$[(\Delta+k^2)^2-2(P-1)]+2[1-\Delta_0(\Delta+k^2)]|Y|^2+\Delta_0^2|Y|^4=0, \tag{15}$$

which is a fairly good approximation to the exact TW solution following from the original Eqs. (3). In terms of the variables used here, the intensity $|Y|^2$ of the exact TWs is given by [18]

$$[(\Delta+k^2)^2-(P^2-1)]+2[1-\Delta_0(\Delta+k^2)]|Y|^2+(1+\Delta_0^2)|Y|^4=0, \tag{16}$$

which in the limit of P close to 1 and large Δ_0 (the scalings used here) gives rise to Eq. (15). We see now the importance of the correct scaling (10) in order to capture the nonlinear resonance: had we used the scaling $\Delta_0=O(1)$ the final result would have been Eq. (14), and consequently, the equation giving the TW intensity would be Eq. (15), making $\Delta_0=0$. This last equation (with $\Delta_0=0$), however, cannot be retrieved from the exact Eq. (16) in the limit $P=1+O(\varepsilon^2)$ and $\Delta_0=O(1)$, and thus the OPE derived with the scaling $\Delta_0=O(1)$ is unable to give sensible results in general, as we already pointed out.

Up to here we have shown that the generalized complex SH equation (13) correctly describes the TWs of OPOs. However, it is important to notice that when TWs are inserted into Eq. (13), the fifth and sixth r.h.s. terms of that equation vanish. Thus in order to investigate the role played by these terms, some solutions different from TWs should be used. As will be reported elsewhere, the fifth r.h.s. term in Eq. (13) is responsible for the destabilization of TWs towards rolls, and the fifth and sixth terms determine the structure and stability of rolls. These predictions are in good agreement with numerical integrations of the original equations [22].

IV. NUMERICS

As evidenced in the previous section two main features in Eq. (13) are to be remarked upon. On the one hand, diffraction is absent in OPOs when the diffraction coefficients of signal and idler fields are equal ($a_1=a_2$; $d=0$), which is a clear difference between OPOs and lasers. On the other hand, the presence of a nonlinear resonance leads to the bistability between the trivial solution and TWs, which, in particular gives rise to localized structures. We illustrate these two properties by numerical calculations in the following subsections.

We have numerically integrated the original microscopic Eqs. (3) by using the split-step technique. In this technique the local terms (pump, losses, nonlinear couplings) are calculated in the spatial domain and the nonlocal terms (diffractive spreading of the three waves) are calculated in the reciprocal wave-number domain. A fast Fourier transform is used to shift from the real space to the wave-number domain, and *vice versa* in every integration step. Periodic boundary conditions have been used in all the calculations. The spatial grids used involved 64×64 pixels.

A. Test of the diffractive character of OPOs: Motion of vortices

An exceptional property of the generalized complex SH equation (13) for OPOs is its ''adjustable'' diffractivity. In the adiffractive limit (equal diffraction coefficients, i.e., $a_1=a_2$) diffraction vanishes and the OPO behaves purely diffusively. This limit can be achieved, e.g., by adjusting cavity losses. It can also be achieved in the case when both signal and idler fields are degenerated in frequency but not in polarization. Far from this limit diffraction can be relatively strong.

We have checked the effect of diffraction through the numerical analysis of the motion of a vortex pair. As follows from the OPE (13), any spatially inhomogeneous structure $y(x,y,t)$ on the top of a TW such as $Y(x,y,t)=y(x,y,t)\exp[i(\omega t+\mathbf{k}\cdot\mathbf{r})]$ propagates, with or without reshaping, with a group velocity $\mathbf{v}_g=2\gamma d\mathbf{k}$ (that propagation manifests itself in the resulting amplitude equation through a term $\mathbf{v}_g\cdot\nabla$). Physically this means that the perturbation is advected by the mean flow (the underlying TW in this case). Since the group velocity is proportional to the diffraction parameter d, a numerical study of the motion of perturbed TWs could be a good check of this analytical prediction. However, since reshaping (and eventually complete disappearance of the perturbation) can in principle occur due to diffusion, sufficiently long lived perturbations must be used. Such a ''stable'' structure is, e.g., an optical vortex [2]. Consequently we have chosen the vortex motion for checking the resulting diffractivity of the OPE. Since the periodic boundary conditions used in the calculations require that the total topological charge be zero in the calculation region, we considered the motion of a vortex pair with opposite topological charges.

Nevertheless the use of vortices can give rise to several complicated motions (radial, tangential, and advection). In order to isolate the advective motion we have located both vortices in such a way (Fig. 1) that the vortices together with their images (due to the periodic boundary conditions) form

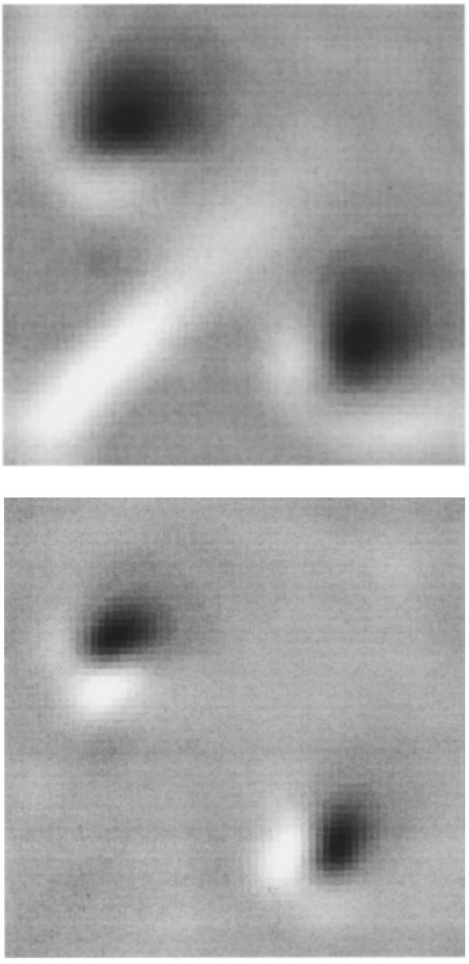

FIG. 1. Snapshots of a moving vortex pair in the signal (top) and idler (bottom) fields. The underlying TWs have a wave number $k=5\pi\sqrt{2}$ and are directed towards the upper-right (signal) and -left (idler) corners. The parameters are $\gamma_0=\gamma_1=\gamma_2=1$, $\Delta_0=0$, $\Delta_1=\Delta_2=-1(\Delta=-1)$, $a_0=0.001$, $a_1=0.0035$, $a_2=0.0005$, and $P=2$. The size of the space domain is 1×1.

a square lattice with alternating charges in space. Then the mutual interactions between vortices and images compensate, and only the basic motion of vortices is due to advection. Such a vortex lattice, although being unstable, is long lived and can ''ride'' for a sufficiently long time on top of the traveling wave.

Figure 1 shows a snapshot of such a vortex pair moving along the diagonal in the up-right direction. As the diffraction parameter d has been chosen to be positive in this case (see caption), motion results along the direction of tilt of the signal TW. The vortices of the idler wave are captured by the signal wave and move in the same direction, although the underlying TW is oppositely tilted [in agreement with Eq. (10)]. Note that the vortices are stretched along the direction of propagation.

Due to the periodic boundary conditions used in the calculations the vortex pair repeatedly passed through the middle of the integration region. The motion of a vortex pair was then followed during typically ten passages, in order to calculate the velocity v_g with sufficient accuracy. In order to make a comparison with the theoretical prediction the space normalization used in Eqs. (3) must be taken into account. In

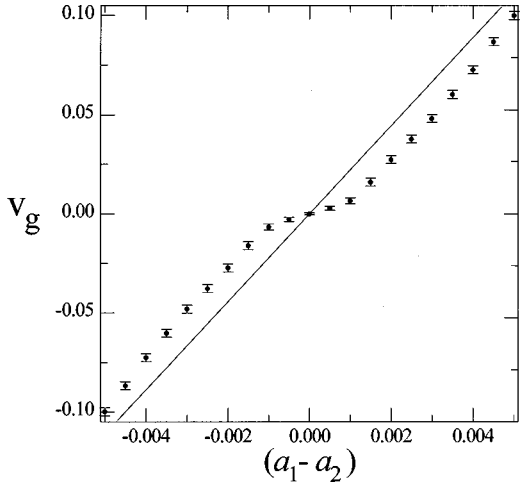

FIG. 2. Velocity of propagation of the vortex pair as a function of a_1-a_2 following from numerical calculations (symbols) and from theory (straight line). Parameters as in Fig. 1.

terms of the unnormalized quantities the velocity is $v_g=(a_1-a_2)k$.

The dependence of v_g on (a_1-a_2) is shown in Fig. 2. Clearly, in the adiffractive limit $(a_1=a_2)$ the vortices are at rest. We also observe that the numerical results closely reproduce the theoretical linear dependence of v_g on (a_1-a_2), except for very small values of (a_1-a_2). Also evident is a nearly constant vertical shift [with the same sign of (a_1-a_2)] that the velocity exhibits not very close to the origin. The behavior close to the origin shows that there exists an additional mechanism for diffraction suppression (the actual velocity is smaller than that predicted by the OPE) beyond that following from the OPE approach.

B. Localized structures via the nonlinear resonance

Another outstanding characteristic of the OPE (13) is the presence of a nonlinear resonance. This phenomenon is present as well in the exact TW solution of the OPO equations as we have stated and gives rise to bistability between the trivial solution (the OPO solution below signal and idler generation threshold) and a TW.

We plot in Fig. 3 the intensity of the signal TW versus its wavenumber k as given by Eq. (16) in order to illustrate the phenomenon. The pump detuning is $\Delta_0=5$. In Fig. 3(a) a negative value of the effective signal detuning $\Delta=-1.5$ has been chosen and consequently the TWs are roughly centered around $k=k_C=\sqrt{1.5}$; see Eq. (4). In Fig. 3(b) $\Delta=1.0$ and TWs exist around $k=k_C=0$. Due to the nonlinear resonance the largest intensity corresponding to a TW does not occur for the linearly resonant wave number k_C but for a different one, as it happens with roll patterns in degenerate OPOs [5]. In all cases, the lower branches of the curves correspond to unstable solutions [18]. Another remarkable consequence of the nonlinear resonance is the possibility of bistability between the trivial and TW solutions. It is easy to show from Eq. (16) that the two conditions for bistability (i.e., for the existence of TWs for pump values below the critical one P_C) are

$$\Delta_0(\Delta+k^2)>1, \tag{17a}$$

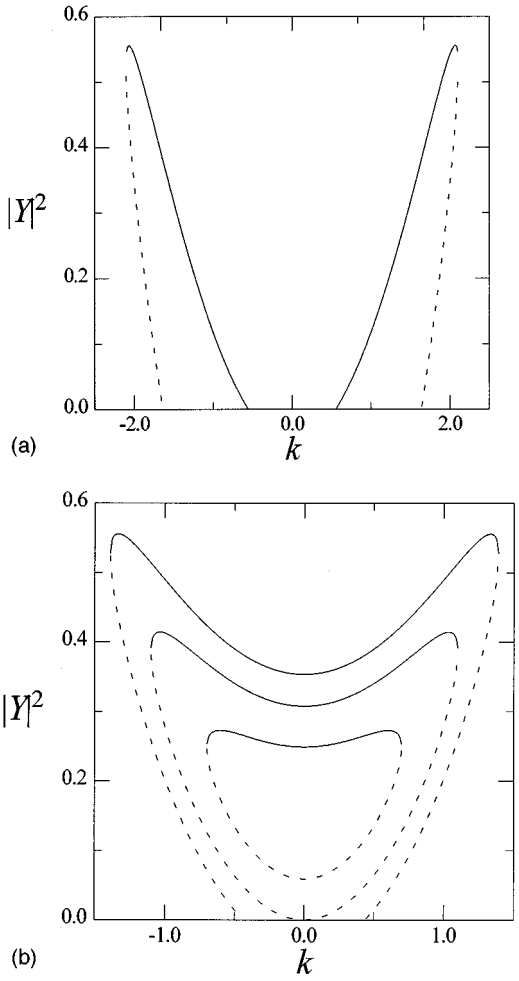

FIG. 3. TW intensity as a function of its wave number k for $\Delta_0=5$, $\Delta=-1.5$ (a) and $\Delta=1$ (b). In (a) $P/\sqrt{2}=1.1$. In (b) $P/\sqrt{2}=0.9$, 1.0, and 1.1 from the inner to the outer curves. Dashed lines indicate unstable branches.

$$\frac{\Delta_0+(\Delta+k^2)}{\sqrt{1+\Delta_0^2}}\equiv P_{\rm lim}<P<P_C\,. \tag{17b}$$

For $\Delta<0$, conditions (17) cannot be fulfilled simultaneously. Contrarily, for $\Delta>0$ it is possible to verify conditions (17): in particular since the lowest $P_{\rm lim}$ corresponds to $k=0$, a sufficient condition for the fulfillement of Eq. (17) is $\Delta_0\Delta>2$, and in this case, at least the on-axis wave ($k=0$) is bistable with the trivial solution in the range given by Eq. (17b). These facts are also illustrated in Fig. 3. The trivial solution is unstable against those k's lying between the cuts of the curves with the horizontal axis $|Y|=0$, and stable against all other k's. Thus in Fig. 3(a) ($\Delta<0$) the trivial solution is unstable with respect to some TWs and stable with respect to others, which leads to the instability of the trivial solution. In Fig. 3(b) ($\Delta>0$) the trivial solution is also unstable for pumps larger than or equal to P_C (the two outer curves, see caption), but stably coexists with TWs for pump values below P_C (the inner curve). It is in cases like the latter one that one can speak of an *absolute bistability*, since the trivial solution is locally stable against any spatial perturbation at the time spatial structures exist. For sure we are not giving here information about the stability of the TWs but there exist parameter settings for which those solutions are stable in the bistability region [18].

But a most important fact related with the nonlinear resonance in Eq. (13) consists in that it affects not only the TW solutions but all spatial structures that may develop in the system. In particular, some of us have recently shown [15] that the nonlinear resonance in degenerate OPOs leads to the appearance of localized structures (LSs). This suggests that this phenomenon could also be present in nondegenerate OPOs. The mechanism of the formation of LSs in this case, as well as in the degenerate OPO, is the bistability between the trivial solution and a spatial structure (TWs in this case, although other structures such as rolls can also be present as we have stated above). Nevertheless, this bistability must be absolute in the sense we have defined above. According to our previous discussion following conditions (17) the absolute bistability is only produced for positive values of the effective detuning parameter Δ and requires a sufficiently large (and positive) value of the pump detuning Δ_0.

Figure 4 displays a series of snapshots showing the development of LSs for $\Delta=1$, $\Delta_0=10$, and $P=1.2$ (which is below the critical pump value, in this case $P_C=\sqrt{2}$, but larger than the lowest $P_{\rm lim}$, which is $11/\sqrt{101}\approx 1.095$). The initial conditions were ''random'' (i.e., generated by a Gaussian distribution of Fourier components, band limited up to some k). In the calculation each sufficiently strong intensity maximum of the random field evolved to a LS. Neighboring LSs annihilated each other during the subsequent evolution, and the number of LSs decreased until eventually a single LS remained (not shown in the figure).

This LS is stable in a relatively large range of pump parameter values, as shown in Fig. 5 where the intensity and width of the LS is plotted as a function of P. Notice that the stability domain of the LS roughly coincides with the domain of bistability between the trivial solution and the TWs (from $P=P_{\rm lim}=1.095$ up to $P=P_C=1.414$, as we indicated).

V. DISCUSSION: WHY SWIFT-HOHENBERG EQUATIONS IN NONLINEAR OPTICS?

Let us go back to the OPE (13) and compare it with the OPE describing the space-time dynamics of degenerate OPOs, derived in Ref. [5]:

$$\gamma^{-1}\partial_t Y=(P-1)Y-Y^3-\tfrac{1}{2}(\Delta-\nabla^2-\Delta_0 Y^2)^2 Y, \tag{18}$$

where all symbols keep the same meaning as in Eq. (13), $\gamma=\gamma_1$, and the field Y is real. Note that Eq. (18) can be mathematically obtained from Eq. (13) by equalizing the parameters of signal and idler fields (in the degenerate case both fields are just the same), which leads to $d=0$ and $\gamma=\gamma_1$ [see Eq. (8)], and imposing the reality of Y.

For the sake of clarity let us concentrate on the case $\Delta_0=0$, in which the equations for both degenerate and nondegenerate OPOs are the real and complex SH equation, respectively. Taking into account that these two equations have been derived for many optical systems, as stated in the Introduction, the central role played by the SH equation in the description of pattern formation in nonlinear optics is evi-

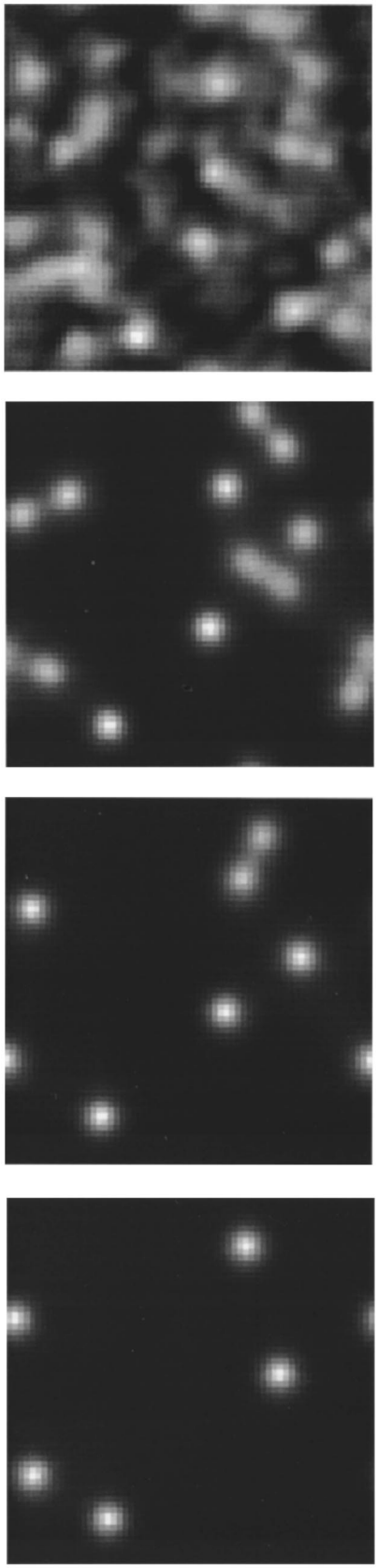

FIG. 4. Ensemble of LSs in the signal field evolving from an initial random field at (from top to bottom) $t=0$, 15, 30, and 90. Parameters are $\gamma_0=\gamma_1=\gamma_2=1$, $\Delta_0=10$, $\Delta_1=\Delta_2=1(\Delta=1)$, $a_0=0.001$, $a_1=0.0025$, $a_2=0.0015$, and $P=1.2$.

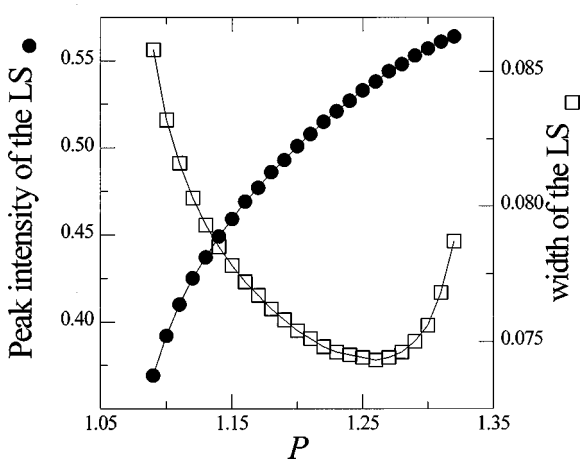

FIG. 5. Intensity at the centre of the LS (filled circles) and its width (open squares) as a function of the pump parameter P. The parameters are as in Fig. 4.

dent, and the following question naturally emerges: why the SH equation in nonlinear optics?

The universal character of the complex SH equation (14) in optics can be understood by noticing that the terms appearing in it describe, in the lowest-order approximation, all the relevant physical phenomena present in most nonlinear optical systems: the first and second terms account for the linear gain and gain saturation, respectively; the last (nonlocal) terms account for the diffraction and the spatial frequency selection, respectively. The role of the nonlocal terms can be understood in the following way: linearization of Eq. (14) around the trivial solution ($Y=0$) with the ansatz $Y(\mathbf{r},t)=y\ \exp(\lambda t+i\mathbf{k}\cdot\mathbf{r})$ leads just to Eq. (7). The real part of λ actually corresponds to a parabolic approximation to the usual Lorentzian gain line profile in the frequency or transverse wave number domains. This phenomenon is well known in nonlinear optics as the (transverse) mode selection. This approximation of the gain profile has a maximum at $k^2=-\Delta$ for negative Δ, which can be understood as the transverse wave number corresponding to a tilted wave, which fits the cavity longitudinal resonance condition. For positive Δ the real part of λ is maximal for $k=0$, and the mechanism of spatial frequency selection cannot take place since the wavelength of the radiation is larger than that of the nearby cavity longitudinal mode [23]. The imaginary part of the growth exponent will be analyzed later.

However, in many cases it is not the complex but the real SH equation [Eq. (18) with $\Delta_0=0$], the one describing a nonlinear optical system. It is evident that some *a priori* relevant ingredients of nonlinear optics are missing here: the originally complex field amplitude has become real, and diffraction has dissappeared. The analysis of all the terms remains as before. In the cases of optical bistability [3,7] the SH equation also contains a constant term, which accounts for the absence of the inversion symmetry $Y\rightarrow -Y$, due to bistability. Which are thus the physical mechanisms leading to the ''strange'' transformation of the initial microscopic equations of some nonlinear optical systems, and which are complex and diffractive, to the real and purely diffusive SH equation? The problem of the vanishing of diffraction has been already pointed out in [3]. There has also been an attempt to explain this in [24], but the actual physical reason

for the dissappearance of diffraction remains unclear.

In order to understand the vanishing of diffraction, we return to the interpretation of the imaginary part of λ. It can be seen from Eq. (7) that diffraction is related to the fact that waves characterized by transverse wave numbers with different moduli k have different eigenfrequencies, governed by the dispersion relation $\omega = d(\Delta + k^2)$, with $\omega = \mathrm{Im}(\lambda)$. Thus, for $d = 0$ (which occurs in the real SH equation, and also in the complex SH equation for OPOs when $a_1 = a_2$) all the perturbations of the trivial solution evolve with the same frequency. This means that in the initial system a frequency locking mechanism must exist. Of course, the concrete mechanism of frequency locking will depend on the particular system. For example, in optical bistability the frequency locking is due to the driving of the injected field, and in the degenerate OPO and degenerate four-wave mixing it is due to energy conservation in the parametric process.

The second restriction that transforms the complex SH equation into the real one is that the order parameter must be real. This restriction means the breaking of the symmetry $Y \to Y \exp(i\phi)$, with ϕ an arbitrary phase, in Eq. (14), which corresponds to the phase locking of the solutions. Obviously phase locking can be incorporated into the complex SH equation through the addition of terms of the type $+\beta(Y^*)^n$ (with β a constant coefficient, and $n = 1,2,\ldots$). Nevertheless in this last case phase locking would not appear at threshold even for $n = 1$. Thus, when a system displays phase locking at threshold (as is the case of, e.g., DOPO and optical bistability) the order parameter must be real.

Thus we can understand the role played by the SH equation in nonlinear optics and, in particular, how diffractive characteristics are lost when a frequency locking exists and how the system can be described by a single real variable when phase locking occurs. Of course, the SH equation (either real or complex) is a skeleton. In each particular case, that equation is generalized in order to accommodate to the specific characteristics of the optical system: inclusion of an additional constant term in optical bistability, inclusion of a nonlinear resonance in degenerate and nondegenerate OPOs, etc.

ACKNOWLEDGMENTS

We gratefully acknowledge S. Longhi for sharing with us Refs. [6] and [16] prior to their publication. This work has been supported by the Spanish DGICYT through Project PB96-0600-C03-01, and by the German Deutsche Fortschungsgemeinschaft.

[1] M. C. Cross and P. C. Hohenberg, Rev. Mod. Phys. **65**, 851 (1993).
[2] P. Coullet, L. Gil, and F. Rocca, Opt. Commun. **73**, 403 (1989).
[3] P. Mandel, M. Georgiou, and T. Erneux, Phys. Rev. A **47**, 4277 (1993).
[4] K. Staliunas, J. Mod. Opt. **42**, 1261 (1995).
[5] G. J. de Valcárcel, K. Staliunas, E. Roldán, and V. J. Sánchez-Morcillo, Phys. Rev. A **54**, 1609 (1996).
[6] S. Longhi and A. Geraci, Phys. Rev. A **54**, 4581 (1996).
[7] V. J. Sánchez-Morcillo and G. J. de Valcárcel, Quantum Semiclassic. Opt. **8**, 919 (1996).
[8] K. Staliunas, Phys. Rev. A **48**, 1573 (1993).
[9] J. Lega, J. W. Moloney, and A. C. Newell, Phys. Rev. Lett. **73**, 2978 (1994); Physica D **83**, 478 (1995).
[10] K. Staliunas, M. F. H. Tarroja, G. Slekys, C. O. Weiss, and L. Dambly, Phys. Rev. A **51**, 4140 (1995).
[11] K. Staliunas, G. J. de Valcárcel, V. J. Sánchez-Morcillo, and E. Roldán (unpublished).
[12] G. L. Oppo, M. Brambilla, and L. A. Lugiato, Phys. Rev. A **49**, 2028 (1994).
[13] G. L. Oppo, M. Brambilla, D. Camesasca, A. Gatti, and L. A. Lugiato, J. Mod. Opt. **41**, 1151 (1994).
[14] M. Brambilla, D. Camesasca, L. A. Lugiato, and G. L. Oppo (unpublished); M. Brambilla, D. Camesasca, and G. L. Oppo (unpublished).
[15] K. Staliunas and V. J. Sánchez-Morcillo, Opt. Commun. **139**, 306 (1997).
[16] S. Longhi, Phys. Scr. (to be published).
[17] S. Longhi, J. Mod. Opt. **43**, 1089 (1996).
[18] S. Longhi, Phys. Rev. A **53**, 4488 (1996).
[19] S. Longhi, J. Mod. Opt. **43**, 1569 (1996).
[20] P. Manneville, *Dissipative Structures and Weak Turbulence* (Academic Press, San Diego, 1990).
[21] Note that Eq. (9) is equivalent to considering that the dynamics of the system only depends on the two slow time scales T_1 and T_2, but not on the ''normal'' time scale t. This means that we are just describing the relevant long-time behavior of the system, dropping all ''fast'' transients that are governed by the rest of eigenvalues given by the linear stability analysis, which are $O(1)$ and negative. See [7] for a more extended discussion.
[22] In Ref. [17] it was concluded that rolls were always unstable in OPOs. This negative result is related to the implicit scaling $\Delta_0 = O(1)$ used in that work (the details will be reported elsewhere).
[23] W. J. Firth and A. J. Scroggie, Europhys. Lett. **26**, 521 (1994).
[24] M. Le Berre, E. Ressayre, and A. Tallet, Quantum Semiclassic. Opt. **7**, 1 (1995).